Ultraviolet-Light-Induced Reversible and Stable Carrier Modulation in MoS_2 Field-Effect Transistors

*Arun Kumar Singh, Shaista Andleeb, Jai Singh, Hoang Tien Dung, Yongho Seo, and Jonghwa Eom**

The tuning of charge carrier concentrations in semiconductor is necessary in order to approach high performance of the electronic and optoelectronic devices. It is demonstrated that the charge-carrier density of single-layer (SL), bilayer (BL), and few-layer (FL) MoS_2 nanosheets can be finely and reversibly tuned with N_2 and O_2 gas in the presence of deep-ultraviolet (DUV) light. After exposure to N_2 gas in the presence of DUV light, the threshold voltages of SL, BL, and FL MoS_2 field-effect transistors (FETs) shift towards negative gate voltages. The exposure to N_2 gas in the presence of DUV light notably improves the drain-to-source current, carrier density, and charge-carrier mobility for SL, BL, and FL MoS_2 FETs. Subsequently, the same devices are exposed to O_2 gas in the presence of DUV light for different periods and the electrical characteristics are completely recovered after a certain time. The doping by using the combination of N_2 and O_2 gas with DUV light provides a stable, effective, and facile approach for improving the performance of MoS_2 electronic devices.

1. Introduction

The identification of graphene as the first two-dimensional (2D) material with exotic electronic, optical and mechanical properties has given birth to research on 2D nanomaterials.[1,2] Graphene has been intensively investigated over the last decade because of its interesting physical properties, chemical properties and technological applications in nanoelectronics, optoelectronics, energy harvesting and sensors.[3–9] Graphene has a conical Dirac spectrum and linear dispersion characteristic.[2] However, the absence of an energy gap in the electronic band structure limits its practical applications in nanoelectronics and optoelectronics.

Dr. A. K. Singh, S. Andleeb, Prof. J. Eom
Department of Physics
and Graphene Research Institute
Sejong University
Seoul 143–747, Korea
E-mail: eom@sejong.ac.kr
Dr. J. Singh, H. T. Dung, Prof. Y. Seo
Faculty of Nanotechnology & Advanced Materials
Engineering and Graphene Research Institute
Sejong University
Seoul 143–747, Korea

DOI: 10.1002/adfm.201402231

Recently, many other 2D materials, such as the transition-metal dichalcogenides, transition-metal oxides and boron nitride, have been investigated.[10–12] Molybdenum disulfide (MoS_2), a layered transition-metal dichalcogenide n-type semiconductor with an indirect bandgap of 1.2 eV (where single-layer (SL) MoS_2 has a direct bandgap of 1.8 eV and bilayer (BL) MoS_2 has an indirect bandgap of 1.3 eV), is attracting increasing interest for its novel electronic and optoelectronic properties.[13–16] Bulk MoS_2 crystal has a structure of interacting layers of a S-Mo-S covalently bonded hexagonal quasi-2D network held together by van der Waals interactions.[17] Thus, SL, BL or few-layer (FL) MoS_2 can be easily fabricated in a similar manner to graphene by mechanical exfoliation.

Nowadays, MoS_2 is incredibly attractive for use in next-generation nanoelectronics and optoelectronics devices because it is a very thin 2D material having a semiconducting nature, an absence of dangling bonds, thermal stability up to 1100 °C, stability in air, no short-channel effect, mobility comparable to that of silicon (in the range of 100–600 $cm^2\ V^{-1}\ s^{-1}$) and a very high on/off current ratio (~10^8).[14,18] MoS_2-based devices such as field-effect transistors (FETs), integrated circuits, photodetectors, memory devices, chemical sensors and supercapacitors have already been demonstrated.[19–26] Among these applications, the FET is the most important and is a basic element of any electronic circuit/device. Presently, researchers are trying to improve the performance of MoS_2 FETs by using different metal contacts (source and drain electrodes), scaling down the device dimensions, using high-*K* materials for the gate dielectric and doping of MoS_2 nanoflakes with self-assembled monolayers or molecules, or with metal nanoparticles.[27–34] It is also reported that doping of two-dimensional materials also enhanced the optical properties and very useful for biological applications.[35,36,41] Doping is the most effective and easy technique for tuning the electrical and optical properties of semiconducting materials. The controlled doping in semiconductor is not only essential for modulating the carrier concentrations and electronic properties but also demanding for fabrication of various complex devices.[42] The reversible and controlled doping of MoS_2 layers, which is of fundamental importance for FET devices, has not yet been well explored.

Here, we present charge-carrier modulation in SL, BL, and FL MoS_2 by N_2 and O_2 gas in the presence of deep-ultraviolet (DUV) light. First, SL, BL and FL MoS_2 are exposed to N_2 gas in the presence of DUV light for different periods. The DUV-light-induced changes in SL, BL, and FL MoS_2 in the presence of N_2 and O_2 gas are investigated by making electrical-transport measurements and performing Raman spectroscopy. The shifting of the threshold voltage towards the negative gate voltage after exposure to N_2 gas in the presence of DUV light reveals the n-doping of SL, BL, and FL MoS_2 FETs. After 30 min exposure to N_2 gas in the presence of DUV light, we expose the same devices to O_2 gas in the presence of DUV light for different periods and observe that the devices completely recover after a certain time. We have found that the recovery time is different for SL, BL, and FL MoS_2 FETs. DUV light in the presence of N_2 gas notably improves the drain-to-source current, carrier density and charge-carrier mobility of SL, BL, and FL MoS_2 FETs.

2. Results and Discussion

We start the fabrication process with the transfer of mechanically exfoliated MoS_2 layers (SL, BL and FL MoS_2) using Scotch tape on a 300-nm SiO_2 substrate with underlying highly p-doped silicon. SL, BL, and FL MoS_2 layers were identified with an optical microscope and through Raman spectroscopy and atomic force microscopy (AFM). **Figure 1** shows optical images of SL, BL, and FL MoS_2 layers and their Raman spectra. The different contrast of MoS_2 flakes on Si/SiO_2 substrate [with the brown background being the Si/SiO_2 substrate] reveals the different thicknesses. On the basis of contrast, we can label the SL, BL, and FL MoS_2 flakes as shown in Figure 1a–c, respectively. Figure 1d displays typical Raman spectra taken for the exfoliated SL, BL and FL MoS_2 layers. Raman spectra of the SL, BL, and FL MoS_2 layers show strong signals from both in-plane E^1_{2g} and out-of-plane A_{1g} vibration. The frequency difference between these two Raman modes varies with layer thickness and can be easily used as a "thickness indicator." The positions of E^1_{2g} and A_{1g} are 385.5 and 404.3 cm^{-1}, respectively, for SL MoS_2. The energy difference between the Raman A_{1g} and E^1_{2g} modes ($\Delta = A_{1g} - E^1_{2g}$) is about 18.8 cm^{-1}, indicating a monolayer. E^1_{2g} and A_{1g} are located at 383.6 and 405.2 cm^{-1}, respectively, and the energy difference (Δ) is 21.6 cm^{-1} for BL MoS_2, confirming the two layers. For FL MoS_2, E^1_{2g} and A_{1g} are located at 382.9 and 407.8 cm^{-1}, respectively, and Δ is 24.9 cm^{-1}. Raman spectra for our SL, BL and FL MoS_2 layers are consistent with those reported elsewhere.[37,38] The thickness of MoS_2 layers was also confirmed by AFM measurements. The thickness of the FL MoS_2 is about 4.6 nm, which indicates seven layers of MoS_2 (Figure S1, Supporting Information).

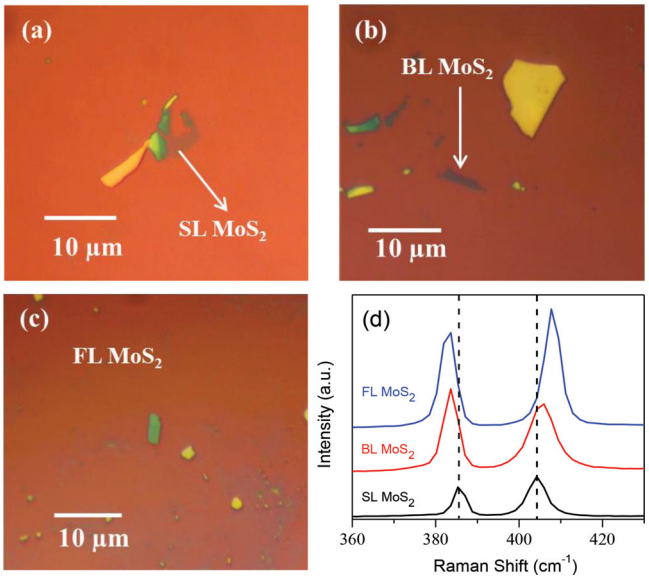

Figure 1. Optical image of the mechanically exfoliated a) SL, b) BL, and c) FL MoS_2 films on Si/SiO_2 substrate. d) Raman spectra of SL, BL, and FL MoS_2 obtained with a 514-nm laser source at room temperature.

Figure 2a shows the schematic cross-sectional view of the structure of a MoS_2 FET. The large patterned electrodes (Cr/Au thickness of 5/30 nm) for SL, BL and FL MoS_2 were made employing photolithography on Si/SiO_2 substrate. The source and drain electrodes of transistors were made employing e-beam lithography, evaporation of Cr/Au (6/80 nm) and lift-off processes. Optical images of the devices are presented in Figure S2 (Supporting Information). All devices were annealed at 200 °C for four hours in a flow of 100-sccm Ar and 10-sccm H_2 to remove the residue and contamination. First, we performed electrical characterizations of our devices at room temperature in a vacuum chamber. Figure 2b–d shows the drain current I_{DS} as a function of the applied back-gate voltage V_g at a fixed drain–source voltage, V_{DS} = 10 mV, for SL, BL, and FL MoS_2 FETs, respectively. The I_{DS}–V_g graph reveals an n-type channel for all SL, BL, and FL MoS_2 FETs. Repeated V_g sweeps on the same device do not show significant variation, while keeping all the voltages constant results in constant I_{DS}. The relations of drain current versus drain–source voltage (I_{DS}–V_{DS}) at various gate voltages (ranging from –8 to +8 V in steps of 2 V) for SL, BL and FL MoS_2 are given in the insets of the respective figures. The linear drain current versus drain–source voltage (I_{DS}–V_{DS}) characteristic of our devices shows good ohmic contact with source and drain electrodes. I_{DS} of our SL MoS_2 device is lower than those of BL and FL MoS_2 FETs, which is consistent with previously reported results.[14,18,27] After characterizations of our pristine devices, we exposed the same devices to N_2 gas in the presence of DUV light for different periods. After 30 min exposure to N_2 gas in the presence of DUV light, we exposed the same devices to O_2 gas in the presence of DUV light for different periods. The doping procedure is detailed in the Experimental section. We made electrical-transport and Raman measurements after each exposure. Before each measurement of electrical transport, we vacuumed the sample chamber for half an hour to remove the atmospheric oxygen. The electrical measurements were made in a vacuum by continuously running a vacuum pump. **Figure 3**a,c,e shows I_{DS} as a function of V_g before and after N_2 and O_2 exposure under constant DUV light treatment for different periods. Figure 3a, c and e clearly shows the shifting of the threshold voltage towards a negative gate voltage with N_2 gas in the presence of DUV light for different periods, which revealed n-doping in SL, BL, and FL MoS_2. We tested several devices and observed the same behavior.

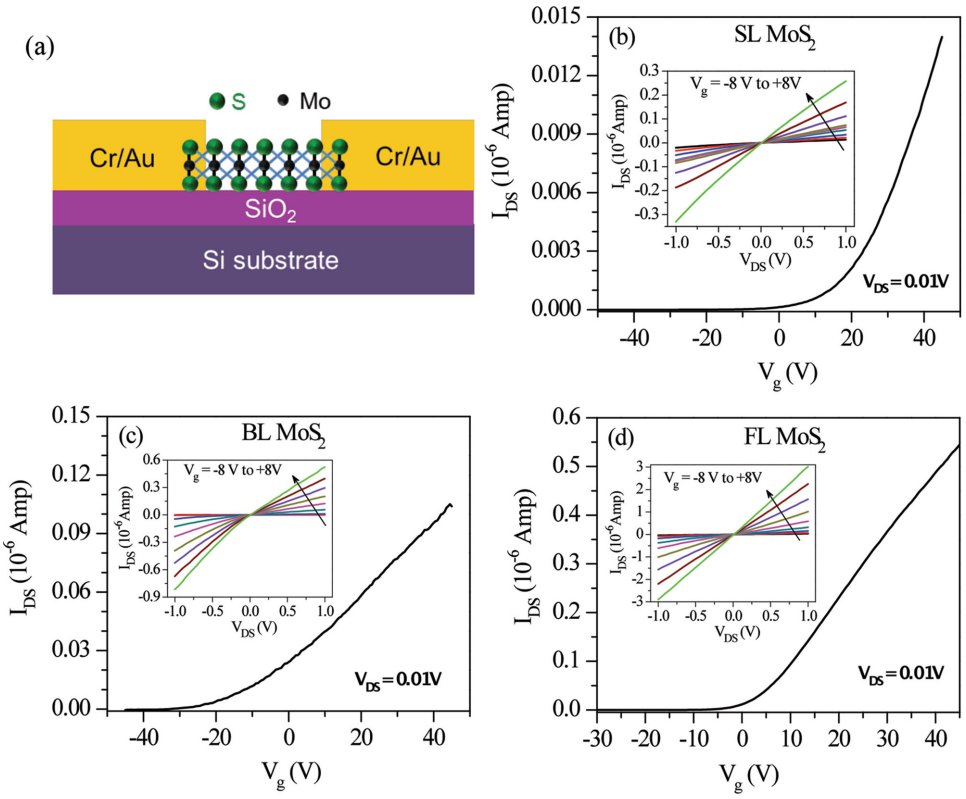

Figure 2. a) Schematic illustration of a MoS_2 transistor. Pristine characteristics of MoS_2 transistors: b) plot of drain current versus back-gate voltage (I_{DS}–V_g) of the SL MoS_2 transistor, with inset showing a plot of drain current versus drain–source voltage (I_{DS}–V_{DS}) at different V_g ranging from –8 to +8 V in steps of 2 V, c) plot of I_{DS}–V_g of the BL MoS_2 transistor, with inset showing a plot of I_{DS}–V_{DS} at different V_g ranging from –8 to +8 V in steps of 2 V, and d) plot of I_{DS}–V_g of the FL MoS_2 transistor, with inset showing a plot of I_{DS}–V_{DS} at different V_g ranging from –8 to +8 V in steps of 2 V.

The n-doping of SL, BL and FL MoS_2 by N_2 gas in the presence of DUV light can be understood in terms of the removal of electron-trapping absorbate groups (such as oxygen or an oxygen-derived group) from MoS_2 nanosheets. The removal of oxygen was also confirmed by energy-dispersive X-ray spectroscopy. The X-rays were scanned on the area of 100 nm × 100 nm on the different locations of all SL, BL, and FL MoS_2 nanosheets. **Table 1** presents the results of the analysis of energy-dispersive X-ray spectroscopy pristine, after DUV+N_2 and after DUV+O_2 treatment for all SL, BL and FL MoS_2 nanosheets. The result of energy-dispersive X-ray spectroscopy shows that significant amount of oxygen was reduced after 30 minute exposure to N_2 gas in the presence of DUV light. However, amount of oxygen was recovered, when we exposed the same devices to O_2 gas in the presence of DUV light for 30 min. The removal of oxygen atoms/molecules from MoS_2 nanosheets significantly increased the drain-to-source current in SL, BL and FL MoS_2 nanosheets. It has been already reported that N_2 gas alone does not affect the electrical properties of MoS_2 nanosheets.[39] However, in our case, N_2 gas in the presence of DUV light notably affected the electrical properties of MoS_2 nanosheets. The n-doping was also observed by Raman spectroscopy as shown in Figure S3 (Supporting Information). After doping through 30 min exposure to N_2 gas in the presence of DUV light, the A_{1g} peak position shifted towards a lower wave number; the shifting of the A_{1g} peak position of n-doped MoS_2 towards a lower wave number has already been reported for other systems.[24,32]

Figure 3b,d,f shows the shifting of the threshold voltage as a function of time of exposure to N_2 and O_2 gas for SL, BL and FL MoS_2, respectively. The threshold voltage of the device is the intercept on the V_g axis obtained by extrapolating the linear portion of the curve of I_{DS} versus V_g to zero I_{DS}. The threshold voltage is found to be –37.4, –40 and –39 V for SL, BL, and FL MoS_2, respectively, after 30 minutes exposure to N_2 gas in the presence of DUV light. We exposed the same devices to O_2 gas in the presence of DUV light for different periods. The threshold voltages shifted towards a positive gate voltage after exposure to O_2 gas in the presence of DUV light, and after a certain period the SL, BL, and FL MoS_2 devices completely recovered. The recovery of MoS_2 devices after exposure to O_2 gas in the presence of DUV may be due to the attachment of oxygen molecules/atoms to MoS_2 nanosheets. There are two possibilities: either oxygen molecules were directly absorbed by MoS_2 nanosheets or oxygen molecules first dissociated into oxygen atoms and the dissociated oxygen atoms then interacted with MoS_2 nanosheets. Oxygen gas molecules can easily dissociate into oxygen atoms under the illumination of DUV light.[43] The interaction of oxygen molecules/atoms takes an electron from MoS_2 nanosheets so that it is p-doped. The p-doping of MoS_2 nanosheets through exposure to O_2 gas has already been reported.[40,41]

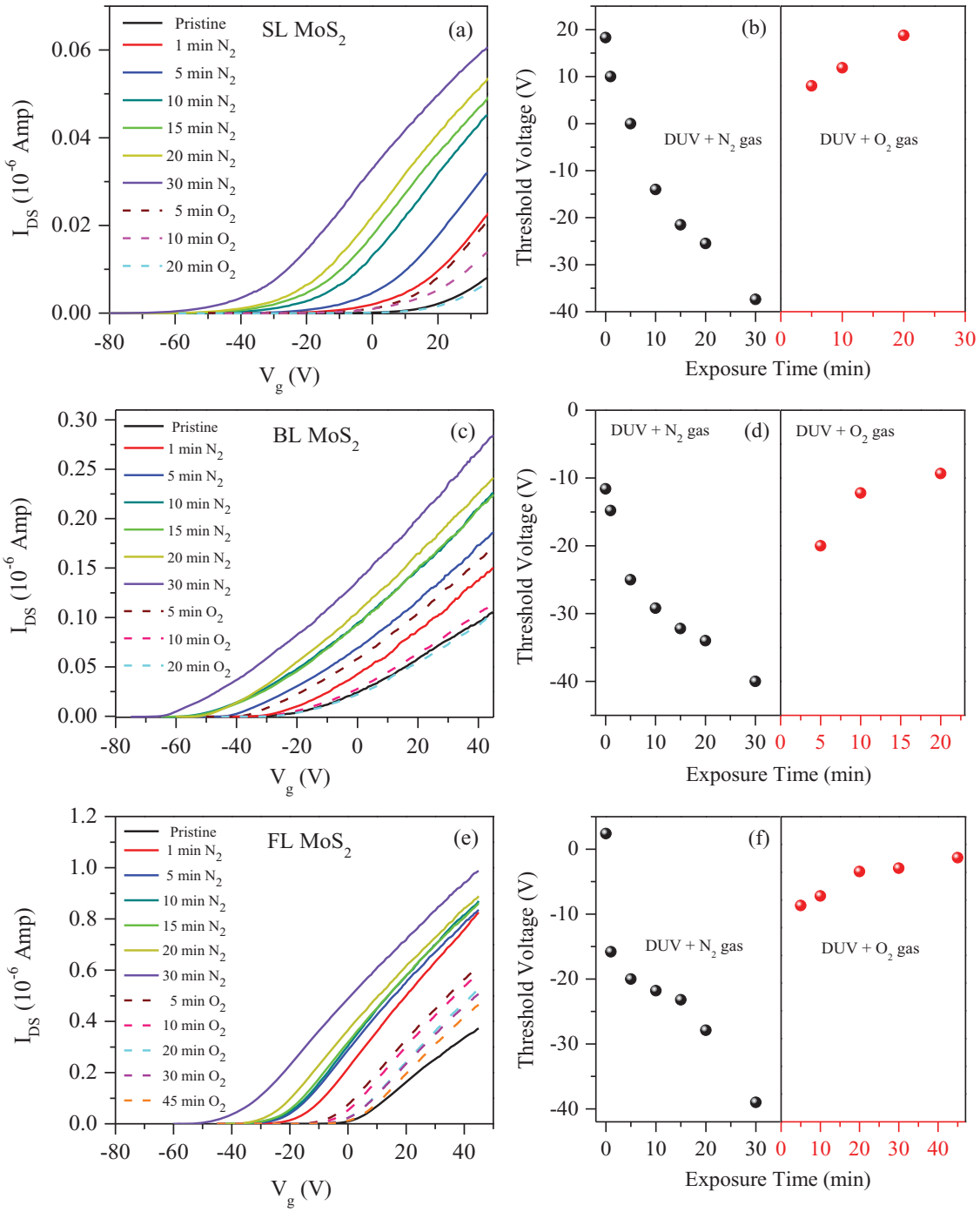

Figure 3. Doping of MoS_2 films by N_2 and O_2 gas in the presence of DUV light. a) Plot of I_{DS}–V_g for different times of exposure to N_2 and O_2 gas in the presence of DUV light and b) the threshold voltage as a function of the time of exposure to N_2 and O_2 gas in the presence of DUV light for SL MoS_2. c) Plot of I_{DS}–V_g for different times of exposure to N_2 and O_2 gas in the presence of DUV light and d) the threshold voltage as a function of the time of exposure to N_2 and O_2 gas in the presence of DUV light for BL MoS_2. e) Plot of I_{DS}–V_g for different times of exposure to N_2 and O_2 gas in the presence of DUV light and f) the threshold voltage as a function of the time of exposure to N_2 and O_2 gas in the presence of DUV light for FL MoS_2.

We also measured I_{DS}–V_{DS} characteristics of SL, BL and FL MoS_2 at different gate voltages for each time of exposure to N_2 and O_2 gas in the presence of DUV light. After exposure to N_2 gas in the presence of DUV light, the drain current (I_{DS}) drastically increased with exposure time. After 30 min exposure to N_2 gas in the presence of DUV light, I_{DS} for SL, BL and FL MoS_2 increased up to ≈50 times with respect to pristine drain current at V_g = +4 V and V_{DS} = 0.5 V. The significant improvement in I_{DS} current is due to the removal of oxygen absorbates from MoS_2 nanosheets and the increase in electron concentrations in the channel region. Another possibility is a higher tunneling probability through the metal–semiconductor interface

Table 1. Energy-dispersive X-ray spectroscopy of SL, BL, and FL MoS_2 nanosheets.

Samples	Element	Pristine	After DUV + N_2	After DUV + O_2
SL MoS_2	O	25.42% ± 0.3%	24.38% ± 0.2%	25.57% ± 0.1%
BL MoS_2	O	26.26% ± 0.1%	25.33% ± 0.5%	26.38% ± 0.3%
FL MoS_2	O	23.61% ± 0.4%	23.08% ± 0.06%	23.50% ± 0.5%

barrier due to lowering of the barrier. The reduction in I_{DS} current after exposure to O_2 gas is due to the absorption of oxygen atoms/molecules into sulfur or defect sites on MoS_2 nanosheets and the trapping of electrons. The I_{DS}–V_{DS} characteristics as functions of exposure time to N_2 and O_2 gas in the presence of DUV light at V_g = +4 V and V_{DS} = 0.5 V for SL, BL, and FL MoS_2 are given in the Supplementary Information (Figure S4, Supporting Information). However, after exposure to N_2 gas in the presence of DUV light, current I_{DS} became weakly dependent on the back-gate voltage (V_g) for SL, BL, and FL MoS_2. This also indicates that SL, BL and FL MoS_2 were heavily n-doped.

Figure 4 shows the mobility and carrier density of SL, BL, and FL MoS_2 as a function of the time of exposure to N_2 and O_2 gas in the presence of DUV light. The mobility of pristine SL, BL and FL MoS_2 is found to be 1.7, 8.1, and 88.8 $cm^2\ V^{-1}\ s^{-1}$, respectively. The mobility of the samples was obtained using the relation $\mu = \frac{L}{C_g W V_{DS}}\left(\frac{\partial I_{DS}}{\partial V_g}\right)$, where L is the channel length, W is the channel width, $\left(\frac{\partial I_{DS}}{\partial V_g}\right)$ is the slope of transfer characteristic of the device, V_{DS} = 0.01 V and C_g is the gate capacitance of ≈115 aF μm^{-2} for our Si/SiO_2 substrate. The mobility of our pristine SL, BL, and FL MoS_2 is higher than values previously reported.[14,21,23,43] The mobilities of SL, BL and FL MoS_2 are significantly improved with exposure to N_2 gas in the presence of DUV light. However, the mobilities of SL, BL, and FL MoS_2 return to the pristine mobility when the devices are exposed to O_2 gas in the presence of DUV light for a certain period. Thus, we can reversibly tune the mobility of MoS_2 through the combination of N_2 and O_2 gas in the presence of DUV light. Figure 4b, d and f shows the carrier density of SL, BL and FL MoS_2 as a function of exposure time to N_2 and O_2 gas in the presence of DUV light. The charge-carrier densities (n) of the devices were estimated using the relation $n = C_g\left(V_g - V_T\right)/e$, where V_T is the threshold voltage of the device, V_g = 30 V and e is the electronic charge. The carrier densities of SL, BL, and FL MoS_2 notably increase with exposure to N_2 gas in the presence of DUV light and reverse back to the pristine state when the devices are exposed to O_2 gas in the presence of DUV light for a certain period, as shown in Figure 4b,d,f.

The stability of doping of 2D nanomaterials is a major issue nowadays, and important to real device applications. We therefore checked the stability of our SL, BL and FL MoS_2 devices after exposure to N_2 gas in the presence of DUV light. To check the stability of doping of MoS_2 layers induced by N_2 gas in the presence of DUV light, we first exposed SL, BL and FL MoS_2 devices to N_2 gas in the presence of DUV light for 30 min and then measured their electrical characteristics. The electrical characteristics of the same devices were measured again after 15 days in atmospheric environments. **Figure 5**a shows the I_{DS}–V_g plots after 30 min exposure of SL, BL, and FL MoS_2 transistors to N_2 gas in the presence of DUV light and the results for the same devices after 15 days. Figure 5a indicates that there were no significant changes in the I_{DS}–V_g plots after 15 days, nor was there much change in the current value of the MoS_2 devices not in threshold voltage. We also checked the stability of the recovered devices. To do so, we first allowed all devices to recover to their pristine state by exposing them to O_2 gas in the presence of DUV light, and then measured their electrical characteristics. The electrical characteristics of the same devices were measured again after 20 days in atmospheric environments. Figure 5b shows the I_{DS}–V_g plots for SL, BL, and FL MoS_2 transistors in a pristine state, and the results for the same devices 20 days later. We observed that there was no significant change in their respective current values, which indicates that our devices are very stable.

3. Conclusion

In summary, we presented reversible charge-carrier modulation in different layers of MoS_2 nanosheets through DUV-light-induced doping. The doping of SL, BL, and FL MoS_2 by N_2 and O_2 gas in the presence of DUV light was investigated by measuring charge transport. SL, BL, and FL MoS_2 were exposed to N_2 gas in the presence of DUV light for different periods, and the shifting of the threshold voltage towards a negative gate voltage revealed the n-doping of all SL, BL, and FL MoS_2 FETs. The n-doped MoS_2 nanosheets completely recovered with exposure to O_2 gas in the presence of DUV light. However, recovery times differed for the SL, BL, and FL MoS_2. The DUV-induced doping by N_2 gas molecules significantly improved the performance of MoS_2 FETs and enhanced device parameters such as the drain current, carrier density and charge-carrier mobility for all SL, BL, and FL MoS_2. Reversible carrier modulation by DUV illumination with gas flow is effective and stable. Our study demonstrated a stable and reversible charge-carrier modulation in MoS_2 nanosheets using DUV light. This allows for new possibilities in relation to doping control using DUV light in MoS_2 nanosheets. Our study may also help improve the performance of other electronic and optoelectronic devices based on MoS_2 nanosheets through the application of DUV light exposure.

4. Experimental Methods

Sample Preparation: SL, BL, and FL MoS_2 films were obtained by micromechanical exfoliation of naturally occurring crystals of molybdenite using adhesive tape and then transferring the MoS_2 layers onto a silicon substrate with a 300-nm oxide layer. Before transferring the MoS_2 layers onto the Si/SiO_2 wafer, the Si/SiO_2 wafer was treated with piranha solution (3:1 sulfuric acid to hydrogen peroxide) for 30 min to remove residual organic contaminants. The numbers of layers in the MoS_2 films were identified by optical microscope and Raman spectroscopy, and confirmed by AFM. The FL MoS_2 had seven layers. Raman spectra were collected at room temperature with a Renishaw microspectrometer having a laser wavelength of 514 nm. To avoid local heating and the introduction of defects by the laser, the laser power was kept at ≈1.0 mW.

Device Fabrication and Measurements: The large patterned electrodes (Cr/Au thickness of 6/30 nm) for SL, BL and FL MoS_2 films were made

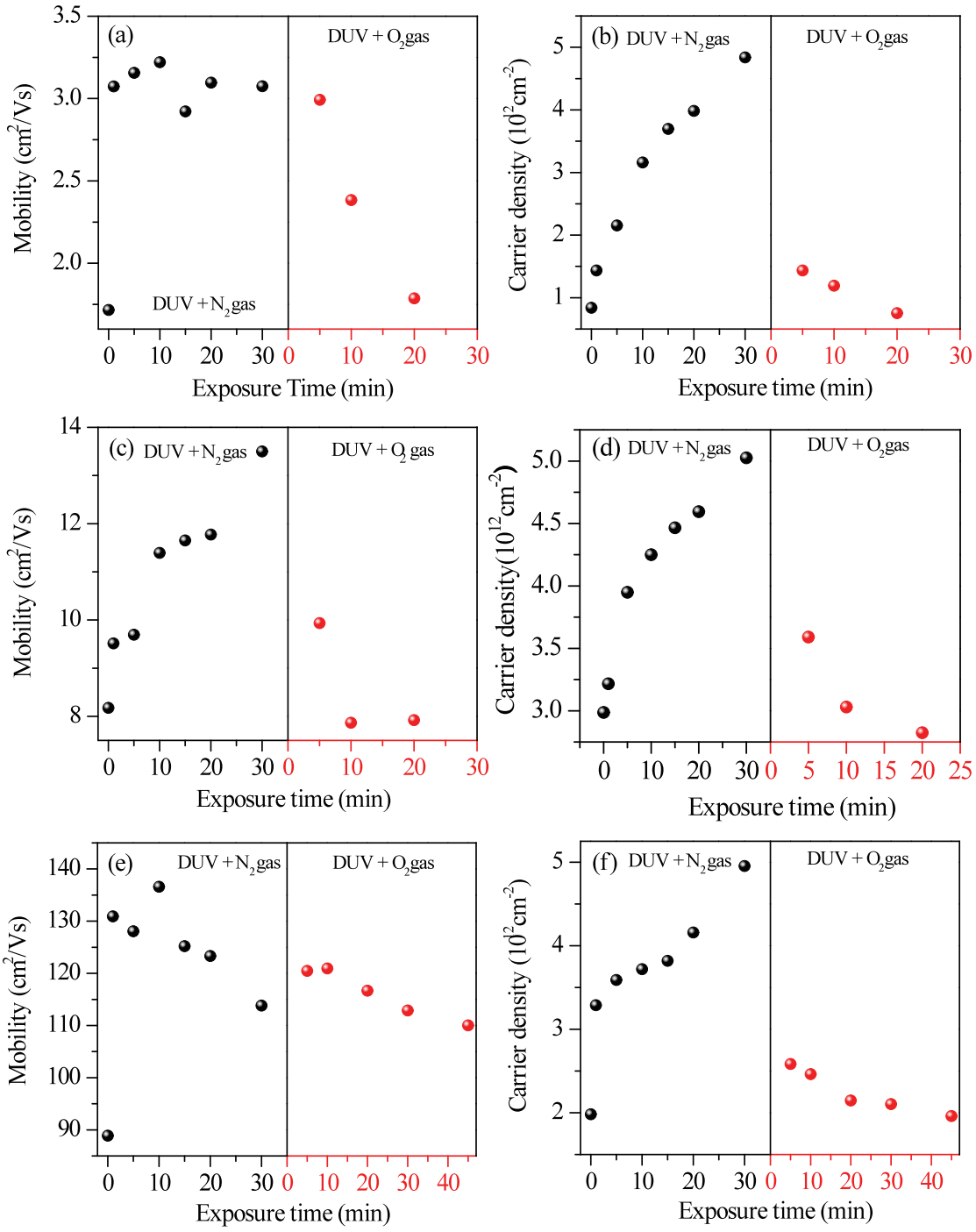

Figure 4. a) Electron mobility and b) charge-carrier density as functions of time of exposure to N_2 and O_2 gas in the presence of DUV light for SL MoS_2. c) Electron mobility and d) charge-carrier density as functions of time of exposure to N_2 and O_2 gas in the presence of DUV light for BL MoS_2. e) Electron mobility and f) charge-carrier density as functions of time of exposure to N_2 and O_2 gas in the presence of DUV light for FL MoS_2.

by photolithography. Source and drain electrodes were patterned employing e-beam lithography and evaporation of Cr/Au (6/80 nm). The channel length of transistors was kept almost constant (≈2.5 μm) for all devices. After device fabrication, all devices were annealed in a tube furnace at a temperature of 200 °C, in a flow of 100-sccm Ar and 10-sccm H_2 for 4 h to minimize the contact resistance of the devices. The devices were electrically characterized using a Keithley 2400 source meter and Keithley 6485 picometer at room temperature in a vacuum.

Ultraviolet-Light-Induced Doping and Characterizations: SL, BL, and FL MoS_2 films were first exposed to N_2 gas flow in the presence of DUV light (λ = 220 nm, average intensity of 10 mW cm^{-2}) for different periods (maximum of 30 min). The same devices were then exposed to O_2 gas flow for different periods in the presence of DUV light. After

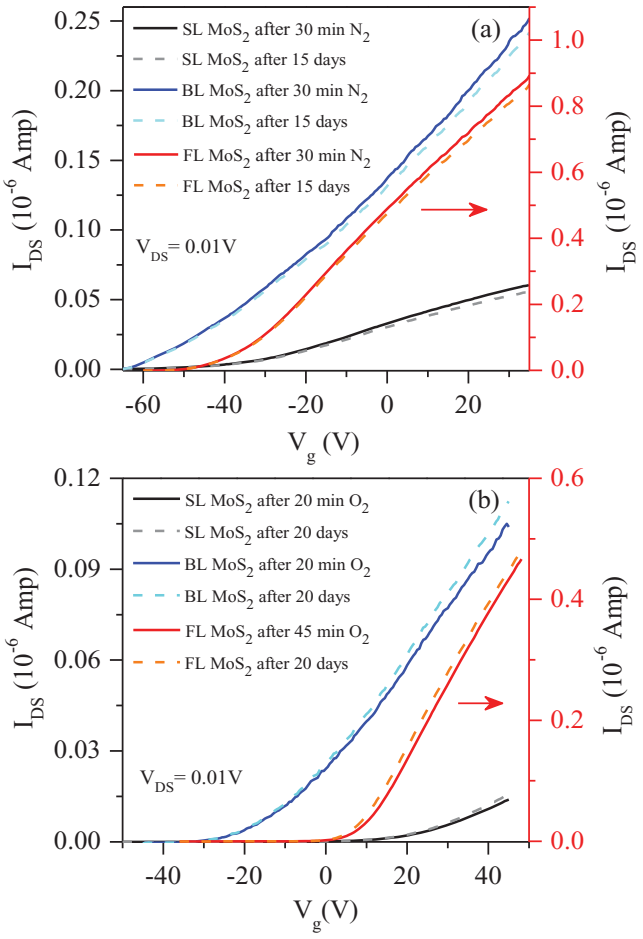

Figure 5. a) Stability of N_2 doping of SL, BL, and FL MoS_2 transistors as revealed by a I_{DS}–V_g plot after 30 min exposure to N_2 gas in the presence of DUV light and a plot for the same devices after 15 days. b) Stability of devices as revealed by a I_{DS}–V_g plot for SL, BL, and FL MoS_2 transistors after recovery with O_2 gas in the presence of DUV light and a plot for the same devices after 20 days.

each exposure to DUV and N_2 or O_2 gas, devices were characterized by Raman spectroscopy and measurements of electrical transport. The sample chamber was vacuum pumped for 30 min before each electrical measurement and during each measurement. All electrical measurements were thus made in a vacuum at room temperature.

Supporting Information

Supporting Information is available from the Wiley Online Library or from the author.

Acknowledgements

This research was supported by the Basic Science Research Program (2010–0020207, 2013R1A1A2061396) through the NRF funded by the Ministry of Education and the Nanomaterial Technology Development Program (2012M3A7B4049888) through the National Research Foundation of Korea (NRF) funded by the Ministry of Science, ICT and Future Planning.

Received: July 6, 2014
Published online: September 12, 2014

[1] K. S. Novoselov, D. Jiang, F. Schedin, T. J. Booth, V. V. Khotkevich, S. V. Morozov, A. K. Geim, *Proc. Nat. Acad. Sci. U.S.A.* **2005**, *102*, 10451.
[2] A. K. Geim, K. S. Novoselov, *Nat. Mater.* **2007**, *6*, 183.
[3] A. K. Geim, *Science* **2009**, *324*, 1530.
[4] J. A. Rogers, *Nat. Nanotechnol.* **2008**, *3*, 254.
[5] P. Avouris, *Nano Lett.* **2010**, *10*, 4285.
[6] S. Pang, Y. Hernandez, X. Feng, K. Müllen, *Adv. Mater.* **2011**, *23*, 2779.
[7] T. H. Han, Y. Lee, M. Choi, S. H. Woo, S. H. Bae, B. H. Hong, J. H. Ahn, T. W. Lee, *Nat. Photonics* **2012**, *6*, 105.
[8] W. Yuan, A. Liu, L. Huang, C. Li, G. Shi, *Adv. Mater.* **2013**, *25*, 766.
[9] A. D. Smith, F. Niklaus, A. Paussa, S. Vaziri, A. C. Fischer, M. Sterner, F. Forsberg, A. Delin, D. Esseni, P. Palestri, M. Östling, M. C. Lemme, *Nano Lett.* **2013**, *13*, 3237.
[10] Q. H. Wang, K. Kalantar-zadeh, A. Kis, J. N. Coleman, M. S. Strano, *Nat. Nanotechnol.* **2012**, *7*, 699.
[11] M. Xu, T. Liang, M. Shi, H. Chen, *Chem. Rev.* **2013**, *113*, 3766.
[12] W. Zhao, Z. Ghorannevis, L. Chu, M. Toh, C. Kloc, P. H. Tan, G. Eda, *ACS Nano* **2013**, *7*, 791.
[13] K. F. Mak, C. Lee, J. Hone, J. Shan,T. F. Heinz , *Phys. Rev. Lett.* **2010**, *105*, 136805.
[14] B. Radisavljevic, A. Radenovic, J. Brivio, V. Giacometti, A. Kis, *Nat. Nanotechnol.* **2011**, *6*, 147.
[15] W. Choi, M. Y. Cho, A. Konar, J. H. Lee, G. Cha, S. C. Hong, S. Kim, J. Kim, D. Jena, J. Joo, S. Kim, *Adv. Mater.* **2012**, *24*, 5832.
[16] S. Balendhran, S. Walia, H. Nili, J. Z. Ou, S. Zhuiykov, R. B. Kaner, S. Sriram, M. Bhaskaran, K. Kalantar-zadeh, *Adv. Funct. Mater.* **2013**, *23*, 3952.
[17] D. Yang, S. J. Sandoval, W. M. R. Divigalpitiya, J. C. Irwin, R. F. Frindt, *Phys. Rev. B* **1991**, *42*, 12053.
[18] S. Kim, A. Konar, W. S. Hwang, J. H. Lee, J. Lee, J. Yang, C. Jung, H. Kim, J. B. Yoo, J. Y. Choi, Y. W. Jin, S. Y. Lee, D. Jena, W. Choi, K. Kim, *Nat. Commun.* **2012**, *3*, 1011.
[19] B. Radisavljevic, M. B. Whitwick, A. Kis, *ACS Nano* **2011**, *5*, 9934.
[20] O. L. Sanchez, D. Lembke, M. Kayci, A. Radenovic, A. Kis, *Nat. Nanotechnol.* **2013**, *8*, 497.
[21] W. Zhang, J. K. Huang, C. H. Chen, Y. H. Chang, Y. Cheng, L. J. Li, *Adv. Mater.* **2013**, *25*, 3456.
[22] S. Bertolazzi, D. Krasnozhon, A. Kis, *ACS Nano* **2013**, *7*, 3246.
[23] H. Li, Z. Yin, Q. He, H. Li, X. Huang, G. Lu, D. W. H. Fam, A. I. Y. Tok, Q. Zhang, H. Zhang, *Small* **2012**, *8*, 63.
[24] D. J. Late, Y. K. Huang, B. Liu, J. Acharya, S. N. Shirodkar, J. Luo, A. Yan, D. Charles, U. V. Waghmare, V. P. Dravid, C. N. R. Rao, *ACS Nano* **2013**, *7*, 4879.
[25] K. Lee, R. Gatensby, N. McEvoy, T. Hallam, G. S. Duesberg, *Adv. Mater.* **2013**, *25*, 6699.
[26] L. Cao, S. Yang, W. Gao, Z. Liu, Y. Gong, L. Ma, G. Shi, S. Lei, Y. Zhang, S. Zhang, R. Vajtai, P. M. Ajayan, *Small* **2013**, *9*, 2905.
[27] S. Das, H. Y. Chen, A. V. Penumatcha, J. Appenzeller, *Nano Lett.* **2013**, *13*, 100.
[28] H. Liu, A. T. Neal, P. D. Ye, *ACS Nano* **2012**, *6*, 8563.
[29] H. Liu, K. Xu, X. J. Zhang, P. D. Ye, *Appl. Phys. Lett.* **2012**, *100*, 152115.
[30] Y. Li, C. Y. Xu, P. Hu, L. Zhen, *ACS Nano* **2013**, *7*, 7795.
[31] H. Fang, M. Tosun, G. Seol, T. C. Chang, K. Takei, J. Guo, A. Javey, *Nano Lett.* **2013**, *13*, 1991.
[32] T. S. Sreeprasad, P. Nguyen, N. Kim, V. Berry, *Nano Lett.* **2013**, *13*, 4434.
[33] Y. Shi, J. K. Huang, L. Jin, Y. Hsu, S. F. Yu, L. J. Li, H. Y. Yang, *Sci. Rep.* **2013**, *3*, 1839.
[34] D. Kiriya, M. Tosun, P. Zhao, J. S. Kang, A. Javey, *J. Am. Chem. Soc.* **2014**, *136*, 7853.
[35] J. Z. Ou, A. F. Chrimes, Y. Wang, S. Tang, M. S. Strano, K. Kalantar-zadeh, *Nano Lett.* **2014**, *14*, 857.

[36] S. Wi, H. Kim, M. Chen, H. Nam, L. J. Guo, E. Meyhofer, X. Liang, *ACS Nano* **2014**, *8*, 5270.
[37] C. Lee, H. Yan, L. E. Brus, T. F. Heinz, J. Hone, S. Ryu, *ACS Nano* **2010**, *4*, 2695.
[38] H. Li, Q. Zhang, C. C. R. Yap, B. K. Tay, T. H. T. Edwin, A. Olivier, D. Baillargeat, *Adv. Funct. Mater.* **2012**, *22*, 1385.
[39] Y. C. Cheng, T. P. Kaloni, Z. Y. Zhu, U. Schwingenschlogl, *Appl. Phys. Letts.* **2012**, *101*, 073110.
[40] W. Park, J. Park, J. Jang, H. Lee, H. Jeong, K. Cho, S. Hong, T. Lee, *Nanotechnology* **2013**, *24*, 095202.
[41] S. Tongay, J. Zhou, C. Ataca, J. Liu, J. S. Kang, T. S. Matthews, L. You, J. Li, J. C. Grossman, J. Wu, *Nano Lett.* **2013**, *13*, 2831.
[42] H. Fang, S. Chuang, T. C. Chang, K. Takei, T. Takahashi, A. Javey, *Nano Lett.* **2012**, *12*, 3788.
[43] H. Qiu, L. Pan, Z. Yao, J. Li, Y. Shi, X. Wang, *Appl. Phys. Letts.* **2012**, *100*, 123104.